

## **Implementation of a New Macroscopic Shear Wall Element**

**Abyaneh, M.H.<sup>1\*</sup>, Vahdani, Sh.<sup>2</sup>, Rahimian, M.<sup>3</sup> and Mansoori, M.R.<sup>4</sup>**

<sup>1</sup> Ph.D. Candidate, School of Civil Engineering, College of Engineering, University of Tehran, Tehran, Iran.

<sup>2</sup> Associate Professor, School of Civil Engineering, College of Engineering, University of Tehran, Tehran, Iran.

<sup>3</sup> Professor, School of Civil Engineering, College of Engineering, University of Tehran, Tehran, Iran.

<sup>4</sup> Assistant Professor, Department of Civil Engineering, Science and Research Branch, Islamic Azad University, Tehran, Iran.

Received: 19 Dec. 2018;

Revised: 26 Aug. 2020;

Accepted: 12 Sep. 2020

**ABSTRACT:** A new macroscopic four node reinforced concrete shear wall element is presented. The element is capable of considering the effect of wall opening without any divisions in the element. Accordingly, the opening may be located arbitrary inside the element. Furthermore, three degrees of freedom are suggested here at each node, totally compatible with the surrounding frame elements. The element is considered only for in-plane stiffness of the wall. Therefore, the surrounding frame elements are assumed to be assembled separately which provides a suitable modeling condition. The element consists of vertical springs, horizontal springs and a shear membrane shell. No rigid element is used in the assembly for imposing the bending action; however, the compatibility is achieved using the definition of shape functions. The element is developed and evaluated in linear applications. The results indicate that some major defects of other macroscopic shear wall elements are removed by the proposed element.

**Keywords:** Finite Element, Four-Node Element, In-Plane Behavior, Macroscopic Model, Membrane Shell, Shear Wall, Vertical and Horizontal Springs.

## **INTRODUCTION**

Reinforced concrete (RC) walls are known as one of the most effective elements in providing resistance against lateral loads induced generally by earthquake or wind. Accordingly, the investigation of the damage to reinforced concrete shear walls is also of great importance, which has been the subject of numerous studies (Naderpour et al., 2017).

The linear and nonlinear behavior of shear wall elements may be properly explained by standard Finite Element procedures based on continuum mechanics (Kotosovos et al., 1992). However, the method leads to very large and expensive models in practical applications and it has been proved that a simplified formulation is needed to predict the wall's overall behavior with reasonable accuracy. These simplified models are

\* Corresponding author E-mail: mabdolla2000@yahoo.com

introduced as macroscopic models, which are suggested by several authors, mostly using several simple elements such as springs and beams (Shin and Kim, 2014; Kolozvari et al., 2018; Rezapour and Ghassemieh, 2018; Wu et al., 2017; Fu, 2020).

In the first macroscopic model, “the equivalent beam model”, wall member is considered as a line element at its centroidal axis which is connected by rigid links to the girders in a wall framed system. The model consists of a flexural elastic member with nonlinear rotational springs at each end for considering inelastic behavior of critical regions (Keshavarzian et al., 1984). The model is presented in common structural platforms such as DRAIN-2DX and SAP2000. Also the model is supported by some codes and prestandards like ASCE 41 (2017) despite its restrictions. The main limitation of this method is that the neutral axis coincides with the center of the wall section. But in reality, the neutral axis changes during the analysis due to cracking and changing the axial force of the wall.

Another macroscopic model was the equivalent truss system. Hiraishi (1983) introduced a non-prismatic truss member on the basis of experimental test results. Mazars et al. (2002) presented a new simplified truss system modeling to simulate nonlinear behavior of shear walls under dynamic loading. They also expressed that by using such modelling method, out of plane flexure and torsion phenomena are also possible. However, the use of this model is limited because of the difficulties in defining the element topology as well as the properties of truss elements. Several investigations have also been done on the different aspects of out of plane behavior in concrete shear walls (Dashti et al., 2014; Saahastaranshu et al., 2017).

The restrictions of the above mentioned models motivated the investigators to formulate more reliable models. Kabeyasawa

et al. (1983) proposed three vertical line element model (TVLEM) to capture the hysteretic behavior of RC walls. In this model, each wall panel in each story is considered as three line vertical elements with infinite rigid beams at the top and bottom of floor levels. Vulcano et al. (1988) extended TVLEM to MVLEM (*multiple vertical line element model*), known as one of the most efficient models introduced so far. In this model the flexural and axial responses of a wall member are simulated by a collection of vertical line elements with rigid beams at the top and bottom story levels, shown in Figure 1. Here, the shear stiffness of wall member is considered by a horizontal shear spring as well. The location of this spring in the height of element is defined by parameter  $c$ . The proper value of  $c$  is based on the expected curvature distribution along the element height. This value is discussed by some researchers (e.g., Vulcano et al., 1988).

MVLEM captures the important features such as shifting of neutral axis as well as the effect of fluctuating axial force on the strength and stiffness which are ordinarily ignored in other macroscopic models. Moreover, the simulation of various material hysteretic models, the effect of confinement on material behavior and nonlinearity of shear behavior are considered in the model. Up to now, many researches have used this model; on the nonlinear behavior of vertical and horizontal springs (Fischinger et al., 1990) and on the coupled walls modeling (Wallace et al., 2006).

In definition of macroscopic element, several requirements should be satisfied in order to make the element accurate, useful and practical. The most important ones are as follows (Fischinger et al., 1990; Wallace et al., 2006; Vulcano et al., 1988):

- 1) The element should be based on a simplified simulation, predicting the wall's overall behavior with reasonable accuracy;

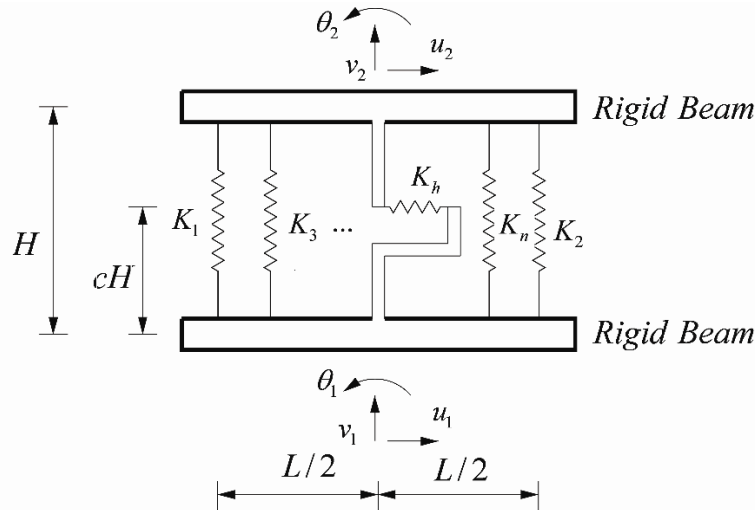


Fig. 1. Multiple vertical line element model (Vulcano et al., 1988)

- 2) The element should produce the resultant internal forces including moment, axial and shear force to be used in design procedure of shear walls according to design codes;
- 3) The element should handle the nonlinear phenomena such as plasticity and concrete cracking;
- 4) The element should be able to consider reinforcements in its linear and nonlinear stiffness;
- 5) The defined degrees of freedom of element nodes should be compatible with other elements, especially with surrounding beams and columns;
- 6) The most important characteristic of the element is its capability of considering the openings without being divided into several elements.

Numerous studies have been conducted on the effect of openings on steel and concrete shear walls (Mahmoudi et al., 2016; Abdollahzadeh et al., 2013). The opening in shear wall has two effects: i) changing the element's stiffness; ii) causing the stress concentrations around the opening. The latter effect is usually handled by code specifications (ACI318M-19) and does not enter the analytical macroscopic model; however, the former should be handled by the element formulation.

Despite performing appropriately in many

applications, MVLEM cannot handle the openings properly. This element handles the opening inside the wall by modeling each pier in each story with a MVLEM element and the coupling beam between two piers with a beam element. Besides, the location of shear spring in height of element is another difficulty in this element.

In this paper, the implemented element is proposed based on MVLEM element with some advancement. Several characteristics of the proposed element are mentioned below:

- 1) The element consists of vertical and horizontal springs and a shear membrane shell, instead of shear spring in MVLEM element.
- 2) It has four nodes with two translational degrees of freedom and one rotational degree of freedom.
- 3) The use of rotational degree of freedom in the presented formulation simplifies the connection of shear wall with other frame elements and causes compatibility of the proposed element with other elements, specially the surrounding beams and columns.
- 4) No rigid element is used in the assembly for imposing the bending action; however, the compatibility is achieved by definition of shape functions.
- 5) The element is considered only for in-

plane stiffness of the wall. Therefore, the surrounding frame elements may be assumed separately.

6) The element considers the openings inside the wall without dividing it to several elements.

Also, it is tried to formulate the element in a way that it can be extended to nonlinear analysis with no restrictions.

**Implemented Macroscopic Wall Element**

The implemented macroscopic wall element consists of vertical springs, horizontal springs and a shear membrane shell, shown in Figure 2. In the proposed model the flexural and axial responses of the wall member are simulated by multiple vertical springs with axial stiffness of  $K_1, K_2, K_3, \dots, K_n$ ; where,  $n$  is the number of vertical springs. Axial stiffness of concrete and steel bars in the vertical direction is considered by these springs.

The horizontal springs with axial stiffness of  $KH_1, KH_2, KH_3, \dots, KH_m$  are added to include the effect of horizontal bars and the beam action in case of walls with opening; where,  $m$  is the number of horizontal springs. The axial stiffness of concrete and steel bars is modeled in the horizontal direction by such springs. The number of springs in both directions is arbitrary and can be increased to obtain more exact results and more refined

description of wall cross section.

Shear membrane shell is used to simulate shear stiffness of the wall member. The horizontal shear spring in MVLEM model is replaced by a shear membrane shell and therefore the parameter  $c$  which defines the location of shear spring in height of element in MVLEM model is omitted.

The element is assembled without using any rigid elements to impose the bending action; however, the compatibility is achieved by definition of the shape functions. This characteristic is another main advantage of the element. Elimination of the rigid beams from the top and bottom of the wall causes implicit compatibility and provides a strong base to use the higher order shape functions, as well as, to add the rotational degree of freedom at each node. These advantages are in the nature of the Finite Element formulation which is presented in the following sections.

The wall element has four nodes, with two translational degrees of freedom and one rotational degree of freedom in each node as shown in Figure 2. This element is very similar to membrane shell element except that the axial and the in-plane shear strains are decomposed here. Replacing the end rigid elements with shape functions has also made the formulation closer to standard Finite Element (Bathe, 2014; Seshu, 2004).

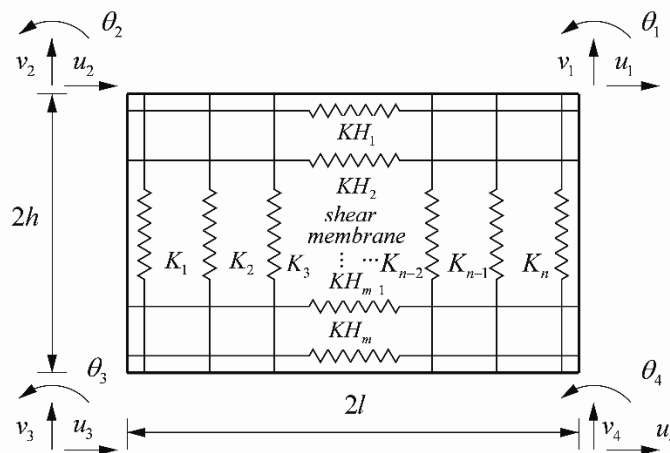


Fig. 2. Implemented macroscopic wall model

**The Element Formulation**

The standard membrane shell element does not consider in-plane rotation and the strain components are related to the translational displacement fields (Bathe, 2014; Seshu, 2004). But beam elements are connected to the shell elements in various cases of structural engineering such as connection of beam to shear wall and moment transfer from beam to shell element is happening. As a result, in-plane rotation is highly required in the numerical models for providing the compatibility of membrane elements with surrounding frame elements. Many authors have established this degree of freedom such as Cook (1986) in rectangular elements. Based on Cook (1986) formulation, the eight-node element with sixteen translational DOFs ( $\bar{u}_i, \bar{v}_i$ ), shown in Figure 3a, is reduced to four-node element with twelve DOFs ( $u_i, v_i, \theta_i$ ), shown in Figure 3b. Translational displacements of nodes with number 1 to 4 are the same in both elements. In the following equations, the displacements of eight-node element are determined based on the displacements of four-node element (Cook, 1986):

$$\bar{u}_{i+4} = \frac{1}{2}(u_i + u_{i+1}) - \frac{y_{i+1} - y_i}{8}(\theta_i - \theta_{i+1}) \quad (1)$$

(For  $i = 4 : i + 1 = 1$ )

$$\bar{v}_{i+4} = \frac{1}{2}(v_i + v_{i+1}) + \frac{x_{i+1} - x_i}{8}(\theta_i - \theta_{i+1}) \quad (2)$$

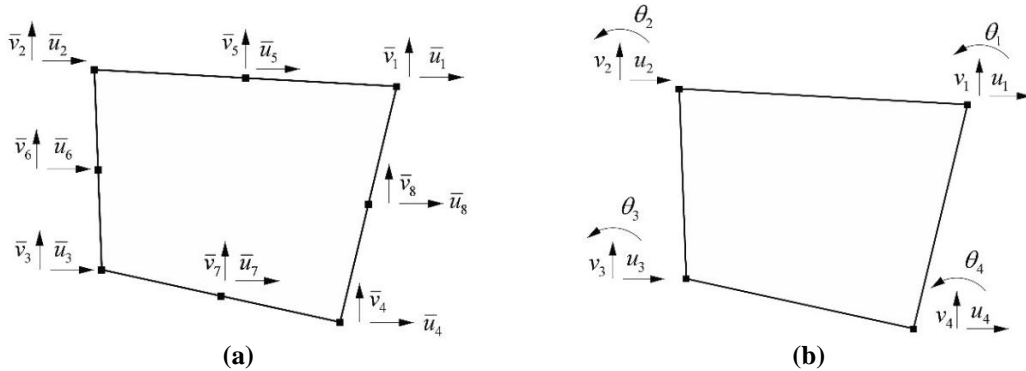


**Fig. 3.** a) Nodal degrees of freedom in eight node element and; b) nodal degrees of freedom in reduced four node element (Bathe, 2014; Seshu, 2004)

where,  $x_i$  and  $y_i$ : are node coordinates.

The nodal displacement vector of four node element is considered as below:

$$\{U\}^T = [u_1 \ v_1 \ u_2 \ v_2 \ u_3 \ v_3 \ u_4 \ v_4 \ \theta_1 \ \theta_2 \ \theta_3 \ \theta_4] \quad (3)$$

Also, nodal displacement vector of eight node element is considered as below:

$$\{\bar{U}\}^T = [\bar{u}_1 \ \bar{v}_1 \ \bar{u}_2 \ \bar{v}_2 \ \bar{u}_3 \ \bar{v}_3 \ \bar{u}_4 \ \bar{v}_4 \ \bar{u}_5 \ \bar{v}_5 \ \bar{u}_6 \ \bar{v}_6 \ \bar{u}_7 \ \bar{v}_7 \ \bar{u}_8 \ \bar{v}_8] \quad (4)$$

By using Eqs. (1-2), nodal displacements of eight node element  $\{\bar{U}\}$  can be found based on nodal displacements of four node element  $\{U\}$ :

$$\{\bar{U}\} = [T]\{U\} \quad (5)$$

where,  $[T]$ : is transformation matrix and expressed as:

$$[T] = \begin{bmatrix} I & \bar{0} \\ L & Q \end{bmatrix} \quad (6)$$

where,  $I$ : is a unit matrix ( $8 \times 8$ ),  $\bar{0}$ : is a null matrix ( $8 \times 4$ );  $L$  and  $Q$ : are defined as follows:

$$[L] = \begin{bmatrix} L_{5,1} & L_{5,2} & 0 & 0 \\ 0 & L_{6,2} & L_{6,3} & 0 \\ 0 & 0 & L_{7,3} & L_{7,4} \\ L_{8,1} & 0 & 0 & L_{8,4} \end{bmatrix} \quad (7)$$

$$[Q] = \begin{bmatrix} Q_{5,1} & Q_{5,2} & 0 & 0 \\ 0 & Q_{6,2} & Q_{6,3} & 0 \\ 0 & 0 & Q_{7,3} & Q_{7,4} \\ Q_{8,1} & 0 & 0 & Q_{8,4} \end{bmatrix} \quad (8)$$

$$[L_{i+4,i+1}] = \begin{bmatrix} \frac{1}{2} & 0 \\ 0 & \frac{1}{2} \end{bmatrix} \quad (9)$$

$$[L_{i+4,i}] = \begin{bmatrix} \frac{1}{2} & 0 \\ 0 & \frac{1}{2} \end{bmatrix} \quad (10)$$

$$[Q_{i+4,i+1}] = -\frac{1}{8} \begin{bmatrix} y_i - y_{i+1} \\ x_{i+1} - x_i \end{bmatrix} \quad (11)$$

$$[Q_{i+4,i}] = \frac{1}{8} \begin{bmatrix} y_i - y_{i+1} \\ x_{i+1} - x_i \end{bmatrix} \quad (12)$$

The isoparametric mapping of the displacements is performed on  $\bar{U}$  components, although the displacement field is expressed in terms of  $U$  components using  $T$  transformation matrix:

$$\{u\} = [\phi][T]\{U\} \quad (13)$$

where,  $\{u\}$ : is displacement vector of a point;  $[\phi]$ : is shape function matrix of isoparametric eight node element.

$$\{u\} = \begin{bmatrix} u \\ v \end{bmatrix} \quad (14)$$

$$[\phi] = \begin{bmatrix} \phi_1 & 0 & \phi_2 & 0 & \phi_3 & 0 & \phi_4 & 0 \\ 0 & \phi_1 & 0 & \phi_2 & 0 & \phi_3 & 0 & 0 \\ 0 & \phi_5 & 0 & \phi_6 & 0 & \phi_7 & 0 & \phi_8 & 0 \\ \phi_4 & 0 & \phi_5 & 0 & \phi_6 & 0 & \phi_7 & 0 & \phi_8 \end{bmatrix} \quad (15)$$

where,  $\phi_1$  to  $\phi_8$  are:

$$\phi_i = \frac{1}{4} (1 + \xi_i \xi)(1 + \eta_i \eta)(-1 + \eta_i \eta + \xi_i \xi) \quad (\text{for } i = 1 \text{ to } 4) \quad (16)$$

$$\phi_i = \frac{1}{2} (1 - \xi^2)(1 + \eta_i \eta) \quad (\text{for } i = 5 \text{ and } 7) \quad (17)$$

$$\phi_i = \frac{1}{2} (1 - \eta^2)(1 + \xi_i \xi) \quad (\text{for } i = 6 \text{ and } 8) \quad (18)$$

where,  $\xi_i$  and  $\eta_i$ : are coordinates of nodes in  $(\xi, \eta)$  system, shown in Figure 4;  $u$  and  $v$ : are the displacement components of a certain point in the element;  $\xi$  and  $\eta$ : are isoparametric coordinates of the point.

The strains of the point are calculated as below:

$$\{\varepsilon\} = [B][T]\{U\} \quad (19)$$

where,  $\{\varepsilon\}$ : is the strain matrix of the point and is achieved as:

$$\{\varepsilon\} = \begin{bmatrix} \varepsilon_x \\ \varepsilon_y \\ \gamma_{xy} \end{bmatrix} \quad (20)$$

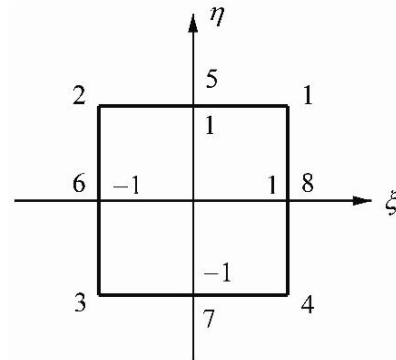


Fig. 4. The coordinates of nodes in  $(\xi, \eta)$  system

where,  $\varepsilon_x$  and  $\varepsilon_y$ : are axial strains of the point in  $x$  and  $y$  directions;  $\gamma_{xy}$ : is shear strain of the point;  $[B]$ : is the standard relation of nodal displacements to strain matrix for isoparametric eight node element:

$$[B] = \begin{bmatrix} \frac{\partial \phi_1}{\partial x} & 0 & \frac{\partial \phi_2}{\partial x} & 0 & \frac{\partial \phi_3}{\partial x} & 0 & \frac{\partial \phi_4}{\partial x} \\ 0 & \frac{\partial \phi_1}{\partial y} & 0 & \frac{\partial \phi_2}{\partial y} & 0 & \frac{\partial \phi_3}{\partial y} & 0 \\ \frac{\partial \phi_1}{\partial y} & \frac{\partial \phi_1}{\partial x} & \frac{\partial \phi_2}{\partial y} & \frac{\partial \phi_2}{\partial x} & \frac{\partial \phi_3}{\partial y} & \frac{\partial \phi_3}{\partial x} & \frac{\partial \phi_4}{\partial y} \\ 0 & \frac{\partial \phi_5}{\partial x} & 0 & \frac{\partial \phi_6}{\partial x} & 0 & \frac{\partial \phi_7}{\partial x} & 0 & \frac{\partial \phi_8}{\partial x} \\ \frac{\partial \phi_4}{\partial y} & 0 & \frac{\partial \phi_5}{\partial y} & 0 & \frac{\partial \phi_6}{\partial y} & 0 & \frac{\partial \phi_7}{\partial y} & 0 & \frac{\partial \phi_8}{\partial y} \\ \frac{\partial \phi_4}{\partial x} & \frac{\partial \phi_5}{\partial y} & \frac{\partial \phi_5}{\partial x} & \frac{\partial \phi_6}{\partial y} & \frac{\partial \phi_6}{\partial x} & \frac{\partial \phi_7}{\partial y} & \frac{\partial \phi_7}{\partial x} & \frac{\partial \phi_8}{\partial y} & \frac{\partial \phi_8}{\partial x} \end{bmatrix} \quad (21)$$

where,  $\frac{\partial \phi_i}{\partial x}$  and  $\frac{\partial \phi_i}{\partial y}$ : are calculated using the following relationships:

$$\begin{bmatrix} \frac{\partial \phi_i}{\partial x} \\ \frac{\partial \phi_i}{\partial y} \end{bmatrix} = [J]^{-1} \begin{bmatrix} \frac{\partial \phi_i}{\partial \xi} \\ \frac{\partial \phi_i}{\partial \eta} \end{bmatrix} \quad (22)$$

where,  $[J]$ : is the Jacobian matrix;  $\frac{\partial \phi_i}{\partial \xi}$  and

$\frac{\partial \phi_i}{\partial \eta}$ : are defined by the equations mentioned below:

$$\frac{\partial \phi_i}{\partial \xi} = \frac{1}{4} (\xi_i (1 + \eta_i \eta) (-1 + \eta_i \eta + \xi_i \xi) + (1 + \xi_i \xi) (1 + \eta_i \eta) \xi_i) \quad \text{for } i = 1 \text{ to } 4 \quad (23)$$

$$\frac{\partial \phi_i}{\partial \xi} = -\xi (1 + \eta_i \eta) \quad \text{for } i = 5 \text{ and } 7 \quad (24)$$

$$\frac{\partial \phi_i}{\partial \xi} = \frac{1}{2} (1 - \eta^2) \xi_i \quad \text{for } i = 6 \text{ and } 8 \quad (25)$$

$$\frac{\partial \phi_i}{\partial \eta} = \frac{1}{4} ((1 + \xi_i \xi) \eta_i (-1 + \eta_i \eta + \xi_i \xi) \eta_i) + (1 + \xi_i \xi) (1 + \eta_i \eta) \eta_i \quad \text{for } i = 1 \text{ to } 4 \quad (26)$$

$$\frac{\partial \phi_i}{\partial \eta} = \frac{1}{2} (1 - \xi^2) \eta_i \quad \text{for } i = 5 \text{ and } 7 \quad (27)$$

$$\frac{\partial \phi_i}{\partial \eta} = -\eta (1 + \xi_i \xi) \quad \text{for } i = 6 \text{ and } 8 \quad (28)$$

$$[J] = \begin{bmatrix} \frac{\partial x}{\partial \xi} & \frac{\partial y}{\partial \xi} \\ \frac{\partial x}{\partial \eta} & \frac{\partial y}{\partial \eta} \end{bmatrix} \quad (29)$$

where,  $\frac{\partial x}{\partial \xi}$ ,  $\frac{\partial x}{\partial \eta}$ ,  $\frac{\partial y}{\partial \xi}$  and  $\frac{\partial y}{\partial \eta}$ : are determined

by defining  $x$  and  $y$  based on shape functions on the node coordinates.

The stiffness matrix of element is calculated as:

$$[k] = \int_A [T]^T [B]^T [D] [B] [T] h dA \quad (30)$$

where  $[k]$ : is the stiffness matrix of the element,  $A$ : is the area of the element,  $h$ : is the thickness of the element and  $[D]$ : is the elasticity matrix. The elasticity matrix has the following form for plane stress problems (Bathe, 2014; Seshu, 2004).

$$[D] = \frac{E}{1-\nu^2} \begin{bmatrix} 1 & \nu & 0 \\ \nu & 1 & 0 \\ 0 & 0 & \frac{1}{2}(1-\nu) \end{bmatrix} \quad (31)$$

According to Eq. (19), shear strain at Gauss points in shear membrane shell and axial strain in each vertical and horizontal spring can be found. The stiffness matrix of element is obtained based on Eq. (30). The shear stiffness of element is obtained by exact integration based on shear term of  $[D]$ . The axial stiffness of the element in both directions is obtained by summing stiffness of vertical and horizontal springs instead of integration on Eq. (30).

It should be noted that in the mentioned formulation, due to the nature of macro elements, the element size has no effect on the results. Several examples with different dimensions of walls and openings are discussed in the following sections which confirm this issue.

### The Element Application in Shear Walls without Opening

Static analysis of a structure is conducted to verify the efficiency and accuracy of the

proposed element where no opening is presented. Figure 5 shows a six-story shear wall with a thickness of 20 cm in all stories and the nodal forces applied to it. In the macroscopic model the two nodes of the bottom of the wall is restrained at horizontal and vertical directions ( $u$  and  $v$ ). Also, each node of the bottom of the wall in the microscopic model is restrained at horizontal and vertical directions.

This structure is analyzed using three approaches:

1. A fine mesh model subdivided into a large number of elements. Analysis of this model is assumed to be the most accurate.
2. MVLEM model.
3. Proposed element.

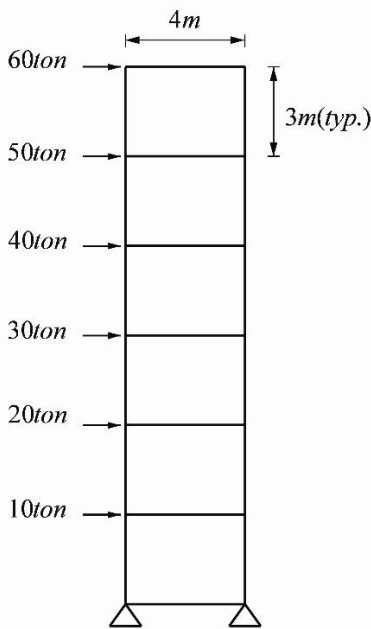


Fig. 5. Example shear wall without opening

Each panel of the wall is simulated as one

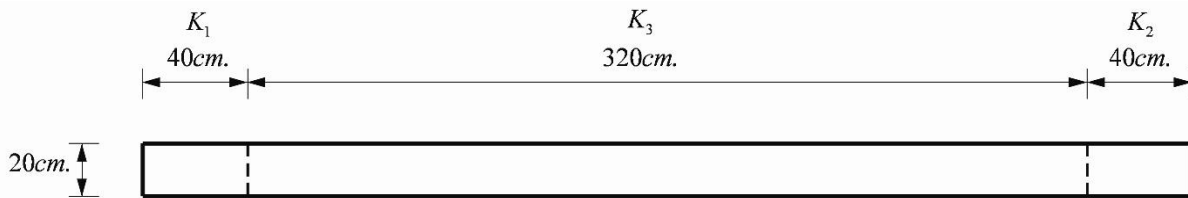
element in each story in both MVLEM model and the proposed element. The structure is also analyzed with different number of springs ( $n$ ) to study the effect of the element subdivisions in both models. Definition of springs is shown in Figure 6 for  $n=3, 6$ .

The lateral displacements of story levels are compared in these three approaches and shown in Figure 7. The vertical displacements of left joints at story levels are also compared in these three approaches and presented in Figure 8.

As it is observed in this example, almost accurate responses are offered by the proposed element for the walls without opening, considering a rational number of springs, like MVLEM model. When number of springs is 3, the error values are high in both macroscopic models; however, the error values are low in both models when number of springs increase to 6. The maximum percent values of errors in vertical and horizontal displacements in both macroscopic models with different spring number are mentioned in Table 1.

Table 1. Comparing the maximum error percentages in proposed element and MVLEM model in the shear wall structure without opening

Model	Horizontal displacement	Vertical displacement
MVLEM (ns=3)	101.3%	102.6%
Proposed element (ns=3)	99.2%	104.3%
MVLEM (ns=6)	3.96%	2.91%
Proposed element (ns=6)	1.93%	2.68%



(a)



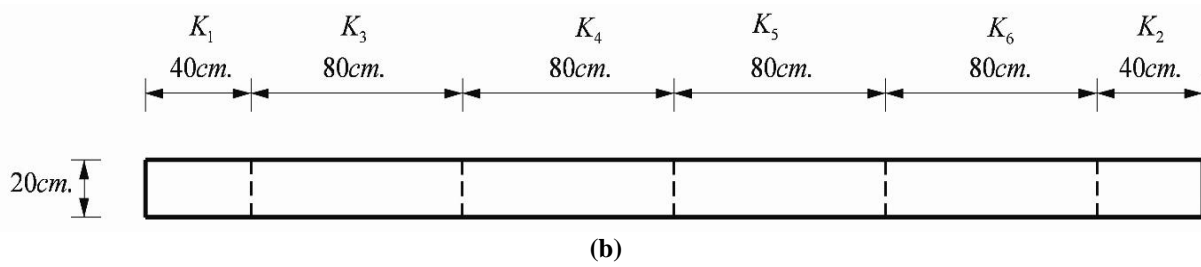


Fig. 6. Definition of springs in MVLEM model and the proposed element when number of springs is: A) 3 and; b) 6

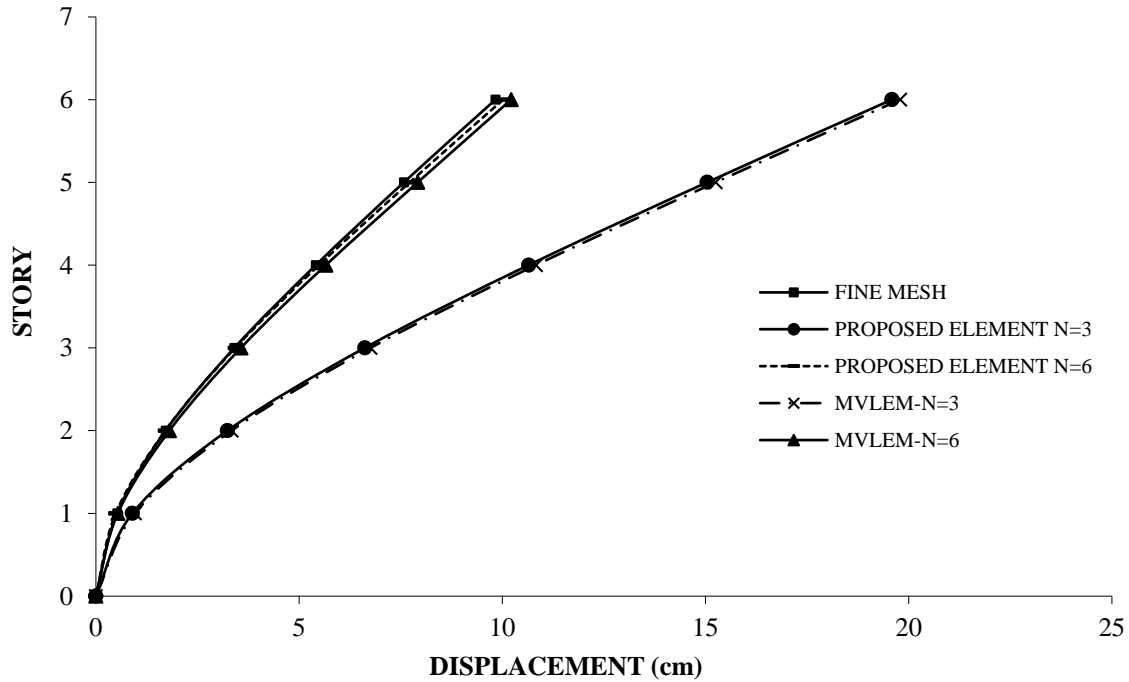


Fig. 7. Lateral displacements of shear wall structure without opening at story levels

### Modeling of Openings

Openings may be formed inside the reinforced concrete walls because of many functional reasons such as doors, windows and ducts. Therefore, the reliable and simplified analysis seems necessary for studying general shear wall structural systems, including openings.

The element, proposed here, can simulate the openings inside the wall without being divided into several elements. Each panel of the wall in each story can be modeled by one element as shown in Figures 9a and 9b. However, MVLEM model as one of the most effective models handles the opening inside the wall by at least three elements (two MVLEM elements and a beam element) in

each panel, shown in Figure 9c. Besides, in modeling by MVLEM element when number of openings is more than one in each panel, the number of elements becomes more as shown in Figure 9d. Therefore, the openings can be modeled more easily by using the proposed element especially in tall and large structures.

Given that in the presence of one opening in each panel, the number of elements of the proposed model is one-third of the MVLEM model; it is estimated that the run time and in-core storage will be reduced to one-third. Obviously, with the increase in the number of openings, the above cases will decrease further.

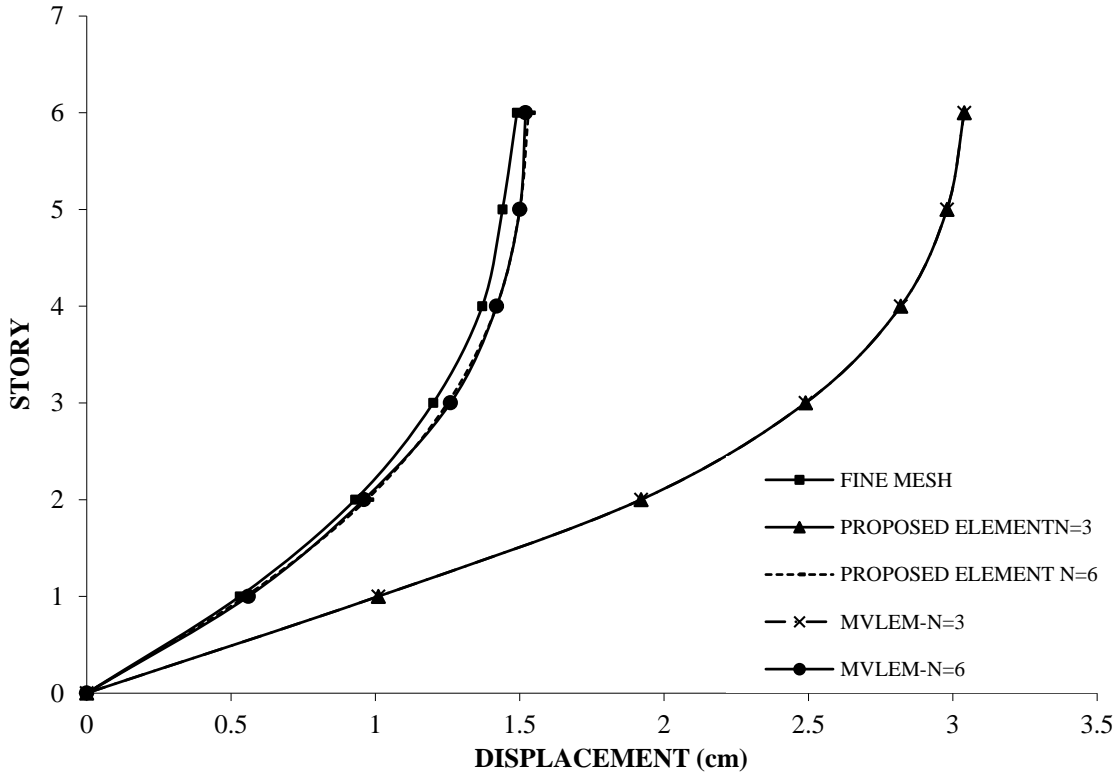


Fig. 8. Vertical displacements of left joints of shear wall structure without opening at story levels

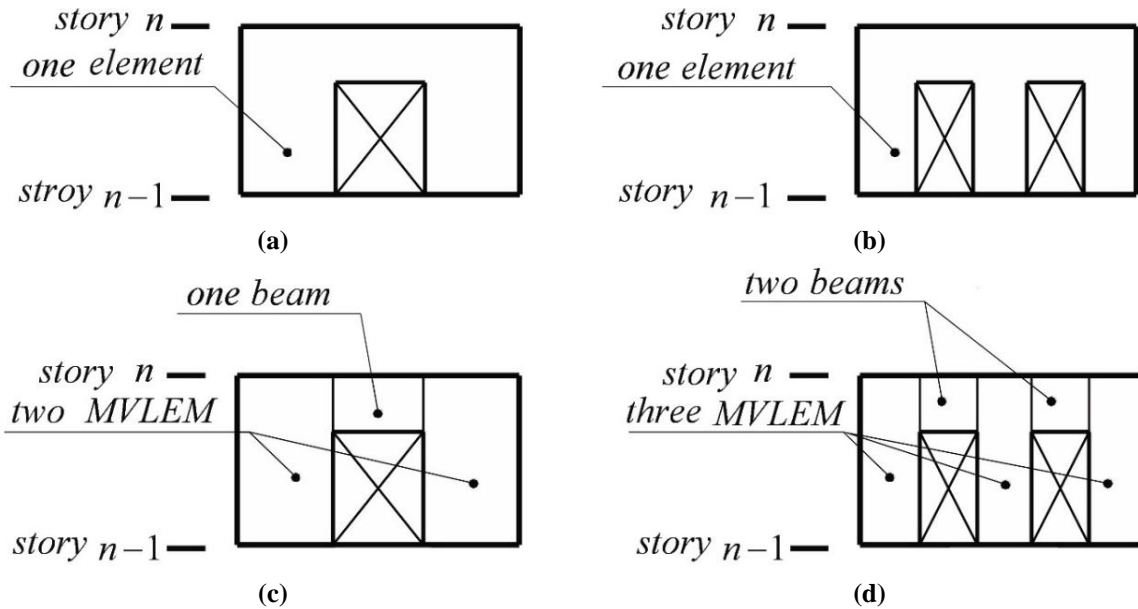


Fig. 9. Modeling of openings with: a) the proposed element (one opening in each panel); b) the proposed element (two openings in each panel); c) MVLEM model (one opening in each panel) and; d) MVLEM model (two openings in each panel)

Here in the proposed element, the vertical and horizontal springs should be omitted in the location of opening for considering the

effect of opening on axial stiffness of wall in both directions, shown in Figure 10.

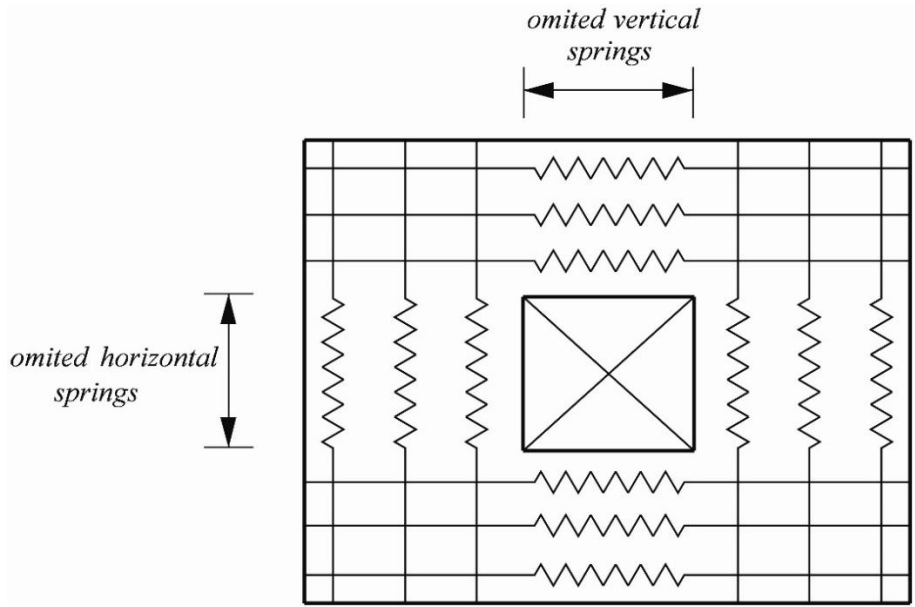


Fig. 10. Modeling vertical and horizontal springs in the proposed element in walls with opening

Moreover, a decreasing shear stiffness coefficient ( $\psi$ ) is defined for concerning the effect of opening on shear stiffness of the wall. This coefficient is considered to be a function of the ratio of opening area to panel area ( $\alpha$ ), the position of opening in X direction ( $\beta$ ) and the position of opening in Y direction ( $\gamma$ ). These three parameters are expressed as below:

$$\alpha = \frac{A'}{A} \quad (32)$$

$$\beta = \frac{l}{L} \quad (33)$$

$$\gamma = \frac{h}{H} \quad (34)$$

where,  $A'$ : is the area of opening;  $A$ : is the area of panel;  $l$  and  $h$ : are the coordinates of the center of opening and  $L$  and  $H$ : are length and height of wall panel as shown in Figure 11.

The effects of these parameters on shear coefficient ( $\psi$ ) were found by numerical tests with different quantities of the parameters. In this paper, some different numerical tests with different values of  $\alpha, \beta, \gamma$  parameters

are performed and the walls are modeled in these tests through two approaches: i) fine mesh model and ii) modeling with the element without any divisions in each panel of the wall. The coefficient ( $\psi$ ) is obtained by equalizing the horizontal displacement results in two ways. These numerical tests indicated changes in  $\beta$  and  $\gamma$  with same  $\alpha$  had no effective change on shear coefficient ( $\psi$ ). Therefore the position of opening in the wall has almost no effect on the shear stiffness of the wall and the opening area is the most effective parameter in shear stiffness of the wall. The variation diagram of shear coefficient ( $\psi$ ) versus  $\alpha$  parameter is shown in Figure 12.

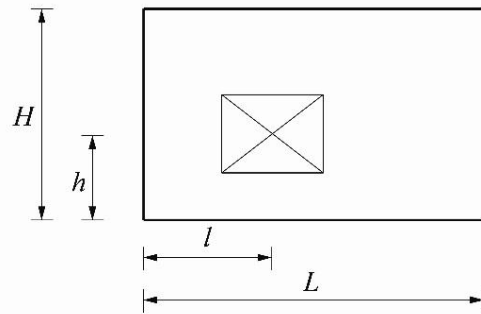


Fig. 11. Defining effective parameters on shear stiffness of the wall with opening

Consequently, modeling of the opening with the presented element includes the following procedures:

- i) The effect of openings is considered by removing the vertical and horizontal springs. Accordingly, all horizontal and vertical springs passing through the range of openings are omitted as shown in Figure 10.
- ii) The ratio of opening area to panel area (Parameter  $\alpha$ ) is calculated based on the geometry of the problem.
- iii) Based on the parameter  $\alpha$  obtained in step 2, the value of  $\psi$  is obtained according to Figure 12.
- iv) Based on the coefficient  $\psi$  obtained in stage 3 the wall shear modulus  $G$  is reduced to  $G'$  ( $G' = G.\psi$ ).

### The Element Applications in Shear Walls with Openings

In this section static analyses are performed on some structures with different openings and different number of stories in order to verify the efficiency and accuracy of the proposed element in term of the ability to consider the opening effects. The example structures are analyzed using three approaches as follows:

1. A fine mesh model subdivided into a large

number of Finite Elements. Analysis of this model is assumed to have the highest accuracy.

2. MVLEM model.
3. The proposed element.

### Shear Wall with Door Type Openings

This example structure is an eight story shear wall with door type openings, shown in Figure 13a. The openings are modeled by MVLEM model and the proposed element, shown in Figures 13b and 13c. The wall model is made by sixteen MVLEM elements in the central axis of each pier and eight beam elements, presented in Figure 13b. The wall model is also simulated by eight proposed elements, shown in Figure 13c. As it is observed in Figures 13b and 13c, the openings are modeled by the proposed element simpler and more realistic compared to MVLEM model. The openings are symmetric to central axis of wall panel. The thickness of the wall is 20 cm in all stories like last example. Three vertical springs (n) are considered for each pier in the proposed element as well as MVLEM model. Furthermore, regarding the element proposed here, four horizontal springs (m) are taken into account for each coupling beam in each story.

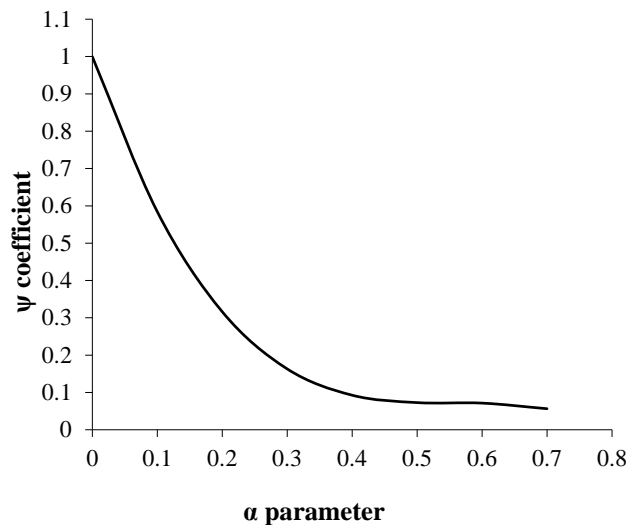


Fig. 12. Variation diagram of shear coefficient ( $\psi$ ) versus  $\alpha$  parameter in the wall with opening

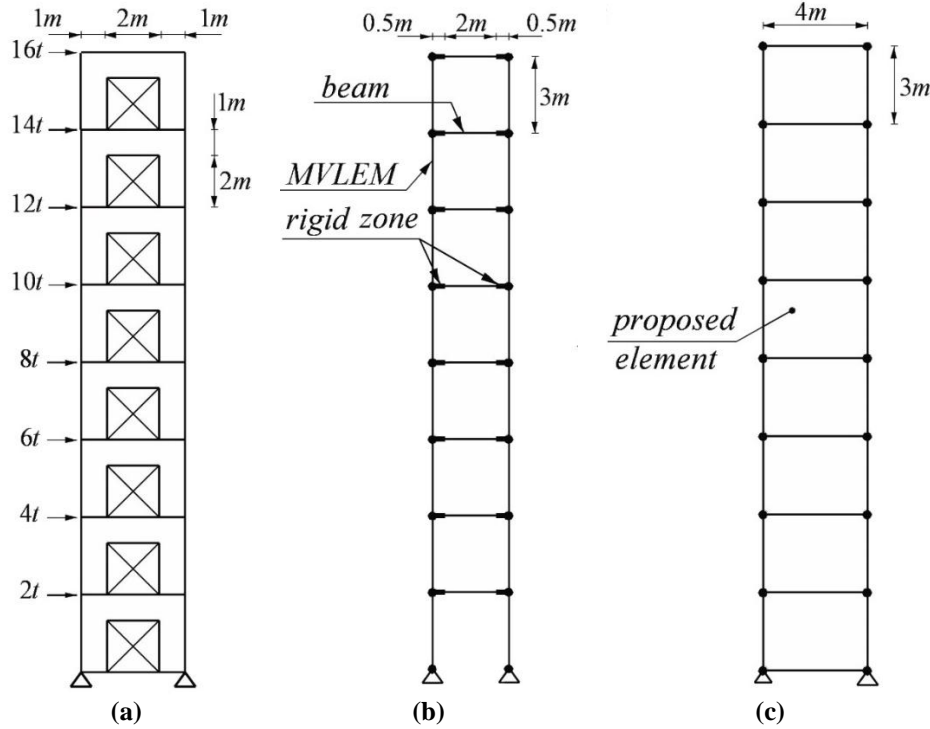


Fig. 13. a) Example shear wall with door type opening; b) modeling of shear wall by using MVLEM elements and; c) modeling of shear wall by using proposed element

The lateral displacements of story levels and the vertical displacements of left joints at story levels are compared in these three approaches and shown in Figures 14 and 15, respectively. As shown in Figure 14, the lateral displacement error of the wall in the case of using the proposed element is less than the MVLEM element in all stories. Figure 15 shows that the vertical displacement in model using the MVLEM element is more accurate than the proposed element from the base to the fourth story. But the proposed element is more accurate from the fourth story to roof. However, the error rate in both models is negligible and the use of the proposed model is preferable due to lesser number of elements.

Maximum percent of errors, occurring in both macroscopic models used for vertical and horizontal displacements are listed in Table 2. As it is observed in this example, the proposed element can model door type openings inside the wall without dividing it into several elements with rational accuracy

in stiffness.

Table 2. Comparing the maximum error percentages in the proposed element and MVLEM model in the shear wall structure with door type opening

Model	Horizontal displacement	Vertical displacement
MVLEM	4.5%	3.7%
	3.9%	3.7%

### Shear Wall with Window Type Openings

This example structure is a seven story shear wall with window type openings in the third, sixth and seventh stories as shown in Figure 16a. Here, the openings are modeled by MVLEM element as well as the proposed element as presented in Figures 16b and 16c. The wall model is made by eleven MVLEM elements in central axis of each pier and two beam elements and eight rigid beams, shown in Figure 16b. The wall model is made by seven proposed elements, as shown in Figure 16c. As it is observed in the figures, the modeling of the openings by MVLEM model is very difficult when the number of the

openings in each panel of wall is more than one and the location of openings differs in the height of wall. On the other hand the modeling of the openings by the proposed

element is very easy. The openings are not symmetric to central axis of wall panel. The wall thickness is 20 cm in all stories like the last example.

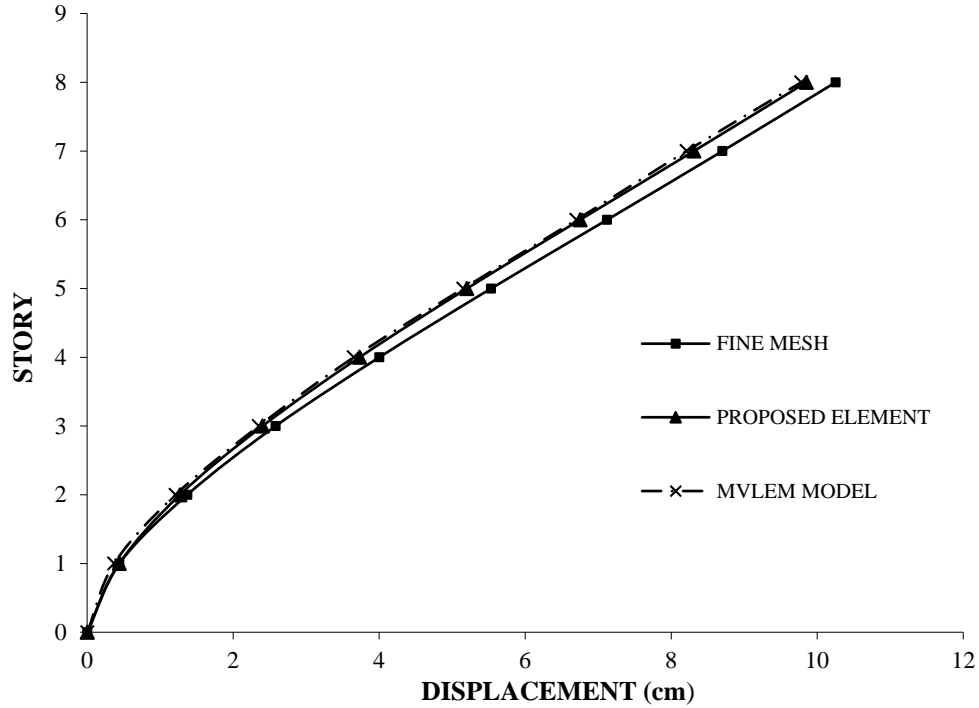


Fig. 14. Lateral displacements in the shear wall structure with door type opening at story levels

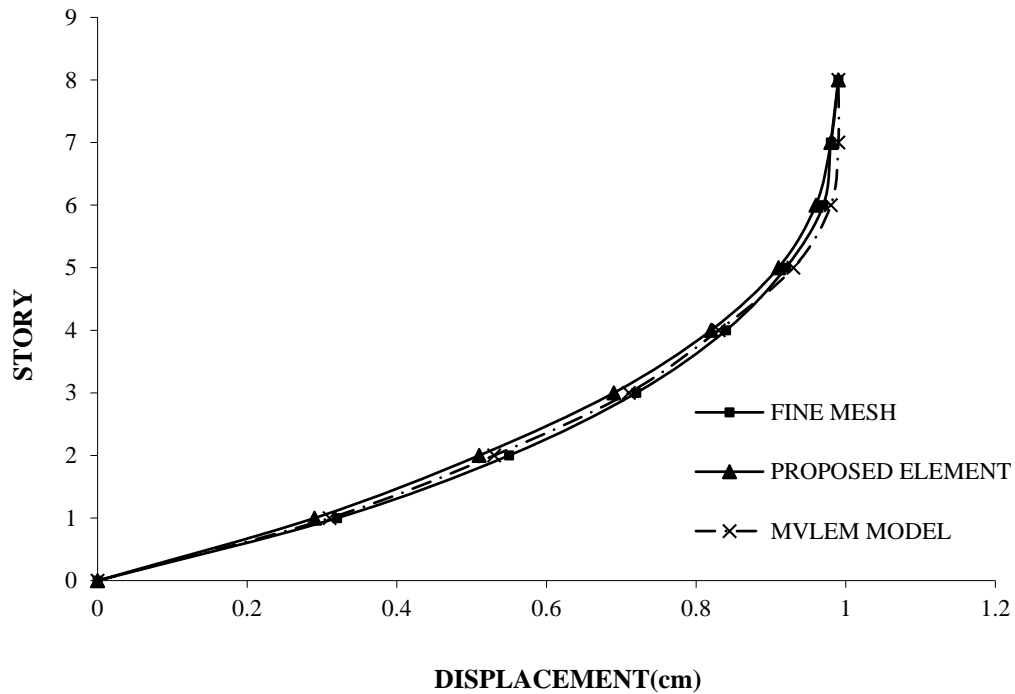


Fig. 15. Vertical displacements of left joints in the shear wall structure with door type opening at story levels

The lateral displacements of story levels are compared using different solutions and are shown in Figure 17. The vertical displacements of left joints at story levels are also compared applying different solutions and are presented in Figure 18. As shown in this figure, the proposed element and the MVLEM element have the same accuracy in estimating the vertical displacement up to fourth story. The MVLEM element is more accurate on the fifth story, but the proposed element is more accurate on the sixth and seventh stories. Here it is also observed that the difference in results with the fine mesh model is negligible.

Maximum percent of errors, occurring in both macroscopic models used for vertical and horizontal displacements are mentioned in Table 3. As it is observed in this example, the proposed element can model easily window type openings which differs the height of wall without dividing it into several elements with rational accuracy in the stiffness. The errors emerged in the model using the proposed element are lower in comparison with those of the model using MVLEM element. This example shows that the type of opening and number of stories

have no effect on the accuracies of the results obtained by proposed method like MVLEM model.

**Table 3.** Comparing the maximum error percentages in the proposed element and MVLEM model in shear wall structure with window type opening

Model	Horizontal displacement	Vertical displacement
MVLEM	2.7%	3.4%
Proposed element	1.8%	1.7%

Table 4 shows the number of elements needed in analysis of the example for different methods. The number of elements in fine mesh model is determined based on the mesh dimensions of about 0.5×0.5 meter. It is observed that if the proposed element is used, the number of elements is significantly reduced compared to the fine mesh method and the MVLEM method, which reduces runtime and in-core storage.

**Table 4.** Comparison of the number of elements needed in different models

Model	Fine mesh	MVLEM	Proposed element
Number of elements	298	21	7

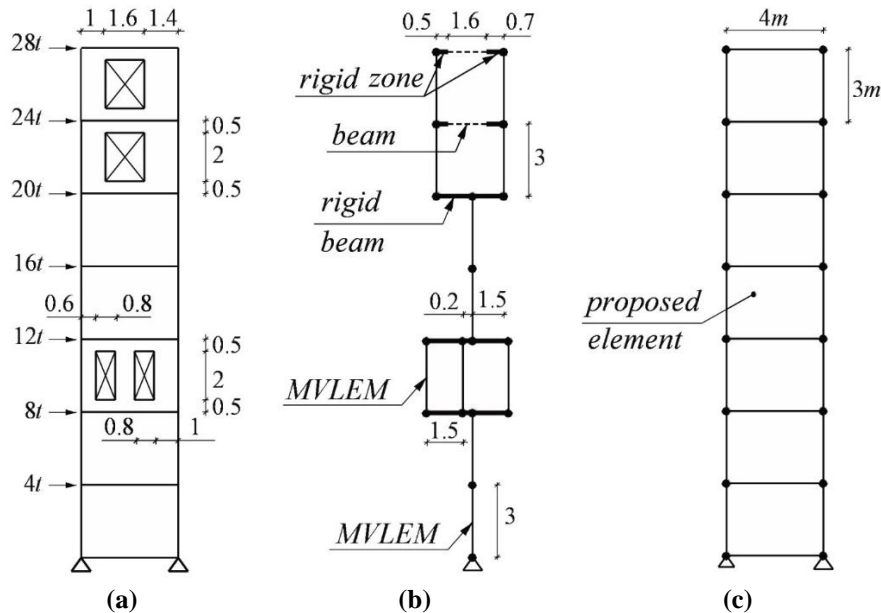


**Fig. 16.** a) Example shear wall with window type opening,; b) modeling of shear wall by using MVLEM elements and; c) modeling of shear wall by using proposed element

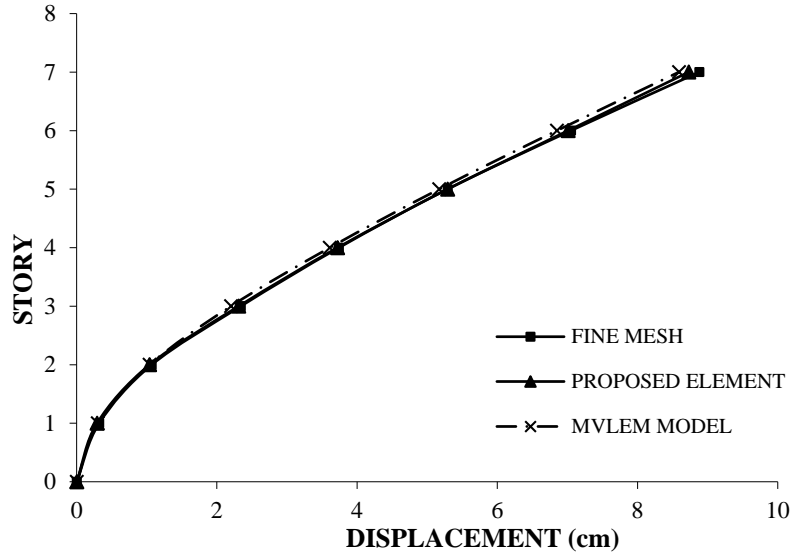


Fig. 17. Lateral displacements of shear wall structure with window opening at story levels

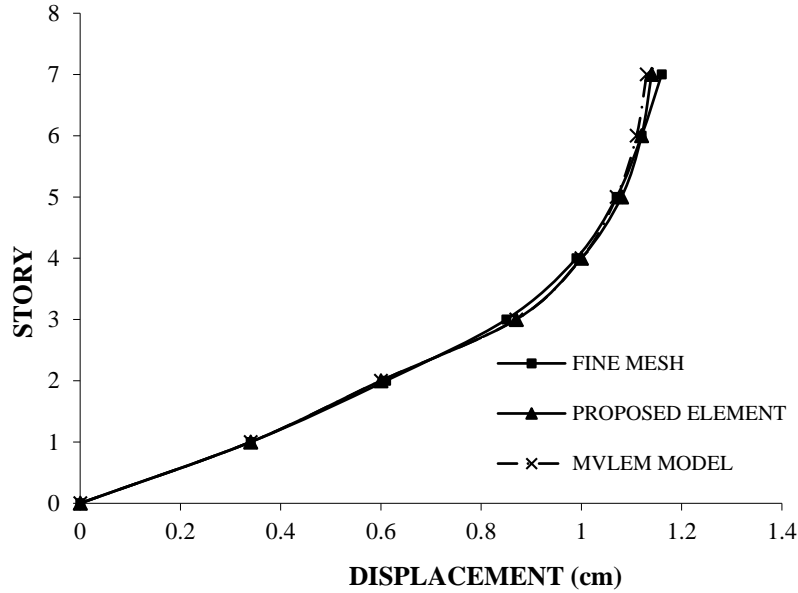


Fig. 18. Vertical displacements of left joints of shear wall structure with window type opening at story levels

### Shear Wall with Opening in Combination with Moment Frame

This example structure is a seven story shear wall in combination with a moment frame structure, shown in Figure 19a. The structure is modeled by MVLEM model and the proposed element, shown in Figures 19b and 19c. The wall model is made by nine MVLEM elements in the central axis of each pier and two spandrel beam elements and two rigid beams, presented in Figure 19b. The

wall model is also simulated by seven proposed elements, shown in Figure 19c. As it is observed in Figures 19b and 19c, the openings are modeled much simpler and more realistic using the proposed element in comparison with MVLEM element. The thickness of the wall is 20 cm in all stories similar to the previous examples. The width of all beams is 40 cm in all stories and the height of beams is 50 cm from first to fourth story and 40 cm from fifth to seventh story.



The width and height of all columns are 50 cm from first to fourth story and 40 cm from fifth story to seventh story. It should be noted that by using MVLEM element, the columns surrounding the wall panel cannot be modeled by frame elements because in this way, both ends of such columns are connected to rigid beams which is different from its real behavior. Consequently, these columns should be modeled by vertical springs that only can consider axial behavior. However, with the proposed element they can be modeled by frame elements like fine mesh model.

The lateral displacements of story levels and the vertical displacements of left joints at story levels are compared in these three approaches. As shown in Figures 20 and 21, the proposed model error in vertical and lateral displacements of the wall is much lower than MVLEM model in all stories. The main reasons for such accuracy are the possibility of modeling the columns surrounding the wall panel as beam elements and considering the rotation degree of freedom of the element nodes using the

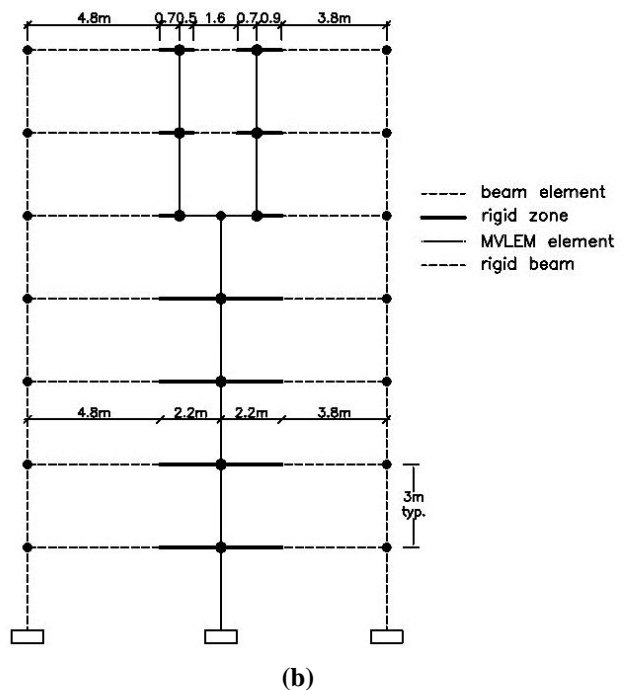
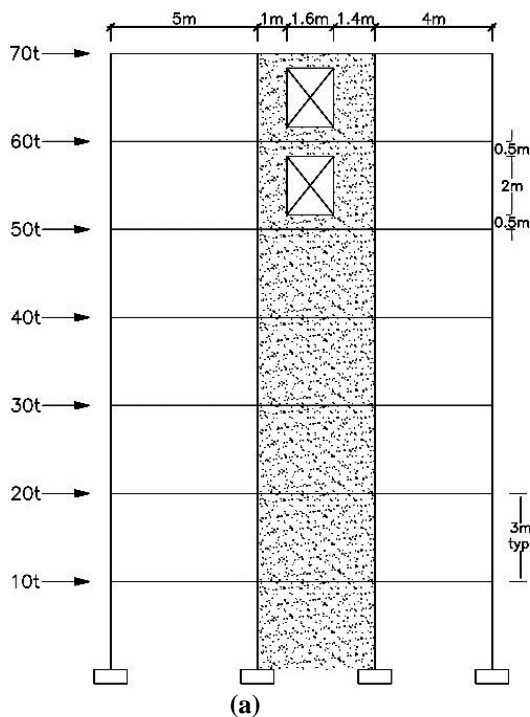
proposed model. Maximum percent of errors, occurring in both macroscopic models used for vertical and horizontal displacements are listed in Table 5.

**Table 5.** Maximum error percentages in the proposed element and MVLEM model in the shear wall structure in combination with moment frame

Model	Horizontal displacement	Vertical displacement
MVLEM	32.1%	22.9%
Proposed element	2.2%	6.1%

**Extending the Formulation to Nonlinear Problems and Out-Of-Plane Behavior**

Several nonlinear phenomena such as: i) plastic behavior of concrete and bars; ii) concrete cracking; iii) separations of bars from concrete; iv) coupling material effect of shear and axial stresses; v) the change in material constant due to confinement and vi) nonlinear shear behavior; are involved in shear wall analysis. As it can be observed, all of these effects are material dependent and some of them such as the first, the second and the sixth play an essential role in analytical response of shear walls.



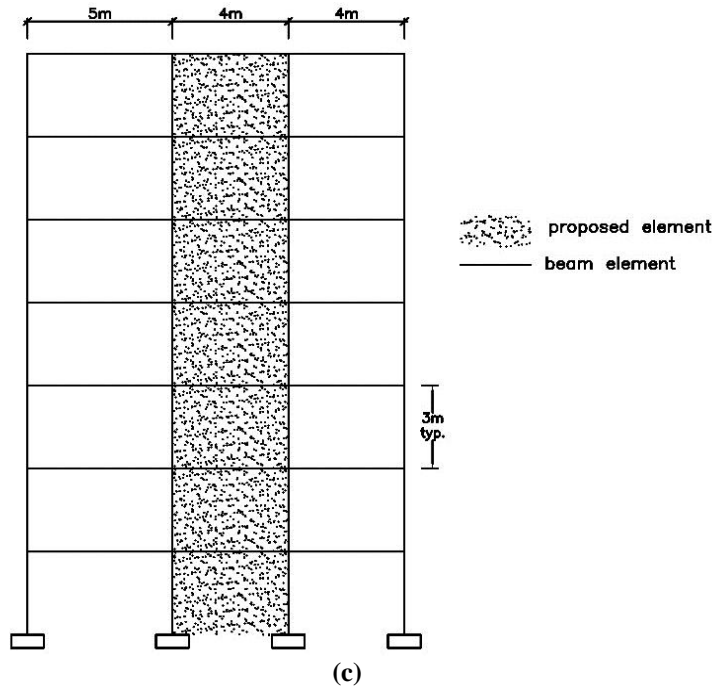


**Fig. 19.** a) Example shear wall with opening in combination with moment frame; b) modeling of the structure using MVLEM element and; c) modeling of the structure using proposed element

The basic formulation of the proposed element may handle the important effects without any major effort. The material constants of the springs are defined separately for each spring either for the concrete or the steel bars. The axial or flexural stiffness of the wall is integrated internally. The cracking of concrete is controlled by the strain level in each panel and is applied in material property of springs. Finally the material can experience the nonlinear shear strength totally independent of axial and flexural one in shear membrane.

Axial nonlinear behaviors of vertical and horizontal springs can be modified by all axial force-deformation relations used in MVLEM model such as axial-element-in-series model (AESM), introduced by Vulcano et al. (1986); modified version of AESM, offered by Vulcano et al. (1988); simplified hysteretic rule, proposed by Fischinger et al. (1990). Also nonlinear flexural or axial response of the wall can be predicted directly by uniaxial material behavior (concrete and steel reinforcement) without incorporating any additional empirical relations.

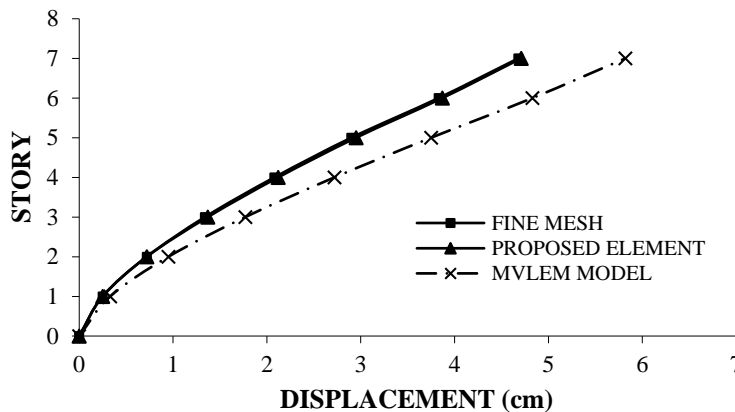


**Fig. 20.** Lateral displacements of the shear wall structure in combination with moment frame at story levels

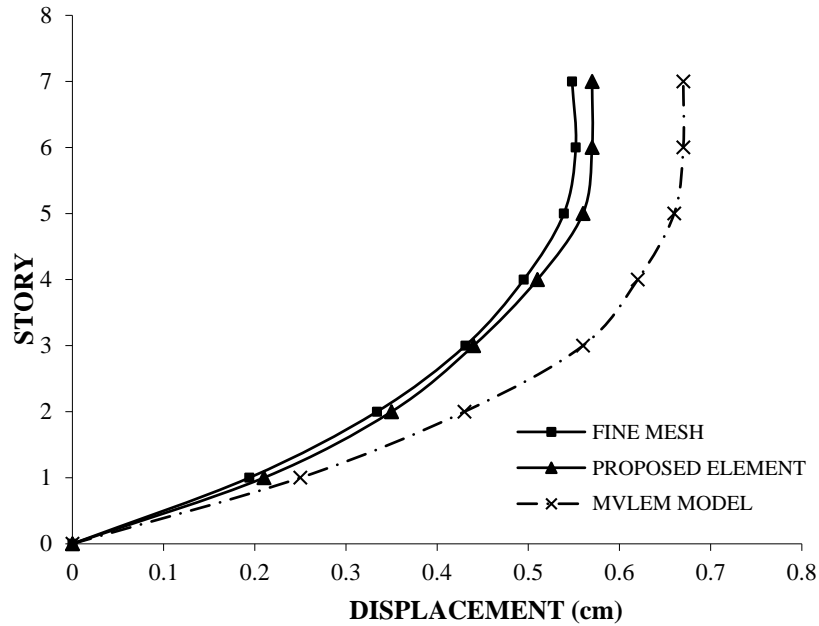


Fig. 21. Vertical displacements of left joints of the shear wall structure in combination with moment frame at story levels

The nonlinear behavior of shear membrane shell can be modified by all shear force-deformation relations used in MVLEM model such as origin-oriented hysteresis model (OOHM) introduced by Kabeyasawa et al. (1983).

The current form of this element cannot handle out of plane behavior and further investigations should be performed to consider such effects.

## CONCLUSIONS

A new microscopic shear wall element is presented in this paper using Finite Element formulation. The main advantages of the proposed elements are discussed as follows:

1. The element is totally compatible with adjacent elements, especially surrounding beams and columns by considering rotation of the element nodes.
2. Pervious microscopic elements such as MVLEM require rigid beams at the top and bottom of the elements, but such beams are removed in the proposed elements.
3. Since horizontal and vertical

reinforcements of the wall are also introduced in the proposed elements by springs, it is possible to consider the effect of reinforcement on the stiffness of the element.

4. The proposed shear wall element does not need to be subdivided in each panel due to better accuracy or existence of the wall opening. Consequently, the number of elements in the shear walls with openings is decreased extremely by using the proposed element which leads to less run time and in-core storage.

5. The effect of opening on the in-plane flexural and axial behavior of the wall is considered by omitting the vertical and horizontal springs in the location of the opening

6. The effect of opening on shear stiffness of the wall is considered by a decreasing coefficient ( $\psi$ ) defined as a function of the ratio of the opening area to the panel area.

7. The element formulation has been made totally compatible with the existing general nonlinear algorithms and it is recommended to be extended to nonlinear problems in the future researches.

8. Results of different examples with different sizes of the elements shows that the proposed element is independent of size effect.

## REFERENCES

- Abdollahzadeh G. and Malekzadeh H. (2013). "Response modification factor of coupled steel shear walls", *Civil Engineering Infrastructures Journals*, 46(1), 15-26.
- ACI318M. (2019). *Building Code Requirements for Structural concrete and Commentary*, American Concrete Institute, Detroit, MI.
- ASCE/SEI 41. (2017). *Seismic evaluation and retrofit of existing buildings*, American Society of Civil Engineers, Virginia.
- Bathe, K. (2014). *Finite Element procedures*, Prentice Hall, Pearson Education, Inc., USA
- Cook, R.D. (1986). "On the Allman triangle and related quadrilateral element", *Computers and Structures*, 22(6), 1065-1067.
- Dashti, F., Dhakal, R.P. and Pampanin, S. (2014). "Simulation of out-of-plane instability in rectangular RC structural walls", *Second European Conference of Earthquake Engineering and Seismology*, Istanbul, Turkey.
- Fischinger, M., Vidic, T., Selih, J., Fajfar, P., Zhang, H.Y. and Damjang, F.B. (1990). "Validation of a macroscopic model for cyclic response prediction of RC walls", *International conference on Computer Aided Analysis and Design of Concrete structures*, Pinerige Press, Swansea, United Kingdom, 1131-1142.
- Fu, W. (2020). "Macroscopic numerical model of reinforced concrete shear walls based on material properties" *Journal of Intelligent Manufacturing*, doi: 10.1007/s10845-014-0879-6
- Hiraishi, H. (1983). "Evaluation of shear and flexural deformations of flexural type shear walls", *Proceedings of the 4<sup>th</sup> Joint Technology Coordination Committee*, U.S. Japan Cooperation, Earthquake Research Program, Building Research Institute, Tsukuba, Japan.
- Kabeyaswa, T., Shioara, H., Otani, S. and Aoyama, H. (1983). "Analysis of the full-scale seven-story reinforced concrete test structure", *Journal of the Faculty of Engineering*, The University of Tokyo, 37(2), 431-478.
- Keshavarzian, M. and Schnobrich, W.C. (1984). *Computed nonlinear response of reinforced concrete wall-frame structures*, Report No. SRS 515, University of Illinois, Urbana, Champaign.
- Kolozvari, K., Arteta, C., Fischinger, M. and Gavridou, S. (2018). "Comparative study of state-of-the-art macroscopic models for planar reinforced concrete walls", *ACI Structural Journal*, 115(6), 1637-1657.
- Kotosovos, M., Povlovic, N. and Lefas, I.D. (1992). "Two and three dimensional nonlinear Finite Element analysis of structural walls", *Proceeding, The Workshop on Nonlinear Seismic Analysis of Reinforced Concrete Buildings*, Elsevier Applied Science, London, 215-227.
- Mahmoudi, M., Mortazavi, M. and Ajdari, S. (2016). "The effect of spandrel beam's specification on response modification factor of concrete coupled shear walls", *Civil Engineering Infrastructures Journals*, 49(1), 33-49.
- Mazars, J., Kotronis, P. and Davenne, L. (2002). "A new modeling strategy for the behavior of shear walls under dynamic loading", *Earthquake Engineering and Structural Dynamics*, 31, 937-954.
- Naderpour, H., Sharbatdar, M.K. and Khademian, F. (2017). "Damage detection of reinforced concrete shear walls using mathematical transformations", *Journal of Structural and Construction Engineering (JSCE)*, 3(4), 79-96.
- Orakcal, K., Wallace, J. and Massone, L. (2006). *Analytical modeling of reinforced concrete walls for predicting flexural and coupled shear flexural responses*, PEER Report C2006/07, University of California, Berkeley.
- Rezapour, M. and Ghassemieh, M. (2018). "Macroscopic modelling of coupled concrete shear wall", *Engineering Structures*, 169(16), 37-54.
- Saahastaranshu, R., Bhardwaj and Amit Varma, H. (2017). "Design of wall structures for in-plane and out-of-plane forces: An exploratory evaluation", *Structures Congress*, Denver, Colorado.
- Seshu, P. (2004). *Textbook of Finite Element analysis*, Prentice-Hall of India Pvt. Ltd; 1<sup>st</sup> Edition, Bombay.
- Shin, J. and Kim, J. (2014). "Different macroscopic models for slender and squat reinforced concrete walls subjected to cyclic loads", *Earthquake and Structure*, 7(5), 877-892.
- Vulcano, A. and Bertero, V.V. (1986). "Nonlinear analysis of RC structural walls", *Proceedings of the 8<sup>th</sup> European Conference on EQ Engineering*, Lisbon, Portugal.
- Vulcano, A., Bertero, V.V. and Colotti, V. (1988). "Analytical modeling of RC structural walls", *Proceedings of the 9<sup>th</sup> World Conference on Earthquake Engineering*, Tokyo-Kyoto, Japan, 41-
- Wu, Y.T., Lan, T.Q., Xiao, Y. and Yang, Y.B. (2017). "Macro-modeling of reinforced concrete structural walls: State-of-the-art", *Journal of Earthquake Engineering*, 21(4), 652-678.